Temperature dependences of structure and physical properties of eutectic InSn49.1 melt

Jie Chen[a]; Fang-Qiu Zu[a]; Zhong-Yue Huang[a]; Zhong-Hua Chen[a]; Qi-Qiang Sun[a]; Xian-Fen Li[a]

[a] Liquid/Solid Metal Processing Institute, School of Materials Science and Engineering, Hefei University of Technology, Hefei 230009, P.R. China

PLEASE SCROLL DOWN FOR ARTICLE

Taylor & Francis
Taylor & Francis Group

Temperature dependences of structure and physical properties of eutectic InSn49.1 melt

Jie Chen, Fang-Qiu Zu*, Zhong-Yue Huang, Zhong-Hua Chen,
Qi-Qiang Sun and Xian-Fen Li

*Liquid/Solid Metal Processing Institute, School of Materials Science and
Engineering, Hefei University of Technology, Hefei 230009, P.R. China*

The temperature dependences of structure and some physical properties of
eutectic InSn49.1 (wt%) melt were investigated by means of high temperature
X-ray diffractometer, internal friction and DC four-probe method. In the heating
procedure of the melt, a discontinuous temperature induced liquid–liquid
structure change was observed within the temperature range of 620–850°C.
The X-ray diffraction results show that both mean nearest neighbour distance
and coordination number altered anomalously within 650–800°C; in addition, the
size of the ordering domain and ordering degree of the melt all decreased
evidently at the end of the structure change. It is presumed that this structure
change resulted from the adjustment of the atomic bonds of Sn–Sn and In–In.
A theoretical discussion on the correlation between structure and physical
properties of InSn49.1 melt was also given.

Keywords: InSn49.1 melt; liquid structure change; physical properties

1. Introduction

It is known that the natures of liquids are recognised as an important but unsolved
problem in many fields [1,2]. Generally, we have the conventional view that a liquid
structure varies gradually with temperature increasing from the melting point to the
gasification point. However, some results in recent works [3–10] suggested that the
structures of some liquid alloys and pure metals (such as Al–Si, Sn–Pb, Ga, Bi, etc) may be
microheterogeneous, and that there exist lots of unsolved microdomains (even particles) in
the melt. Investigation of these microdomains showed that the microheterogeneous states
are metastable or non-equilibrium thermodynamically, and microdomains would dissolve
within specific temperature ranges. Moreover, in our former works [11,12], by means of
X-ray diffraction, temperature induced discontinuous liquid–liquid structure changes
were observed in InSn80 and InSn20 melts, but the temperature dependences of the liquid
structure and physical properties of eutectic InSn49.1 melt are still not clear.

Eutectic InSn49.1 alloy is widely applied in the electronic industry as one type of
Pb-free solders, and for those solders, good wetting behaviour and high strength are

---

*Corresponding author. Email: fangqiuzu@hotmail.com

very important. It is known that the alteration of the liquid structure could affect the interatomic binding force, and further influence the wetting behaviour of the melt. In addition, due to the hereditary effects of liquids on solids, the melt thermal history has great effect on microstructures and properties of the alloys. Therefore, a study on the structure of liquid eutectic InSn49.1 alloy could be of great importance for improving the wetting behaviour and strength of the In–Sn solder.

In this article, the temperature dependences of the structure and some physical properties (internal fiction, electrical resistivity and thermopower) of eutectic InSn49.1 melt are investigated. The aims of the present work are to study how the melt structure changes as the continuous temperature elevates, and to gain more information about the relationships between the atomic structure and physical properties of liquid alloys.

2. Experimental details

2.1. *X-ray diffraction measurements*

X-ray diffraction (XRD) measurements were carried out using a θ–θ type liquid metal X-ray diffractometer. The details of the XRD measurements are the same as described elsewhere [11,12], and the data processing method is the same as in [11].

2.2. *Internal friction measurements*

The sample of InSn49.1 alloy used in this work was prepared from pure tin and indium granules of high purity ($5N$), held at $600°C$ for $210\,min$ under the shielding slag (B_2O_3), and then solidified for use. The details of the internal friction apparatus and measurements are the same as we had described in [13,14]. With given torsion frequency (f) and constant amplitude, the energy dissipation $Q^{-1}(=\tan \Phi)$ of the melt was measured as a function of temperature, where Φ is the phase angle at which the strain lags the given persistent oscillating stress.

2.3. *Electrical resistivity and thermopower measurements*

The electrical resistivity ρ and thermopower S of the liquid alloy were measured by the DC four-probe method. The experimental details have been described elsewhere [15,16]. The InSn49.1 sample was prepared with pure tin and indium granules of high purity ($5N$). The melt was heated to $600°C$ and held for $210\,min$ under the shielding slag (B_2O_3), and then poured into a quartz cell and cooled to the temperature below liquidus for the following experiments. In the resistivity measurements, the heating and cooling rate were both $3°C\,min^{-1}$, and the ρ–T curve was recorded by a computer datum collection system.

3. Results and discussion

Figures 1 and 2 show the structure factors $S(Q)$ and the pair distribution functions $g(r)$ of the InSn49.1 melt, respectively. In order to reveal the structural changing pattern of the melt better, the temperature dependences of r_1 and N_1 were calculated and shown in Figure 3. As a whole, the magnitude of N_1 nearly has no variation except an obvious change between $650°C$ and $800°C$. And it seems likely that r_1 decreased abruptly within
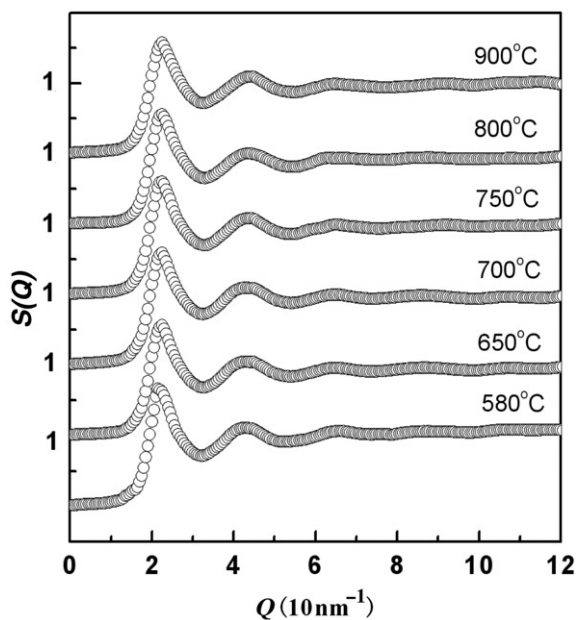
Figure 1. Total structure factors $S(Q)$ of molten InSn49.1 at different temperatures.
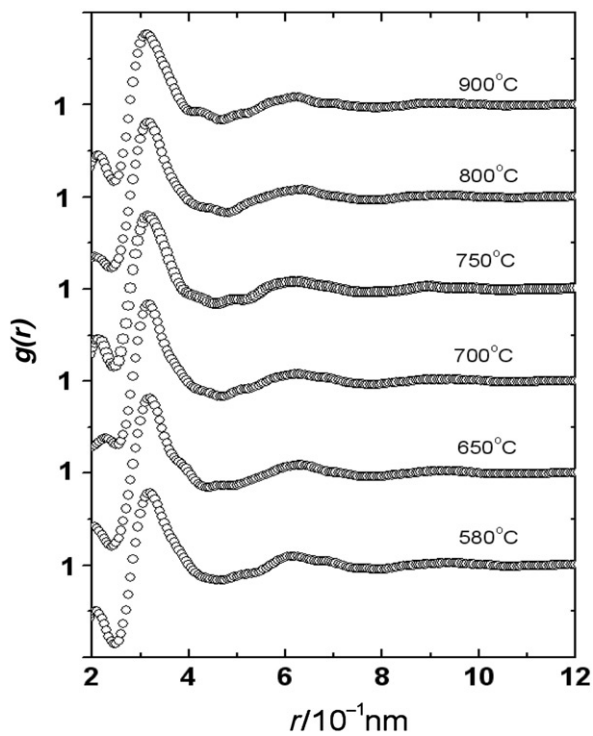

Figure 2. Pair distribution functions $g(r)$ of InSn49.1 melt at different temperatures.
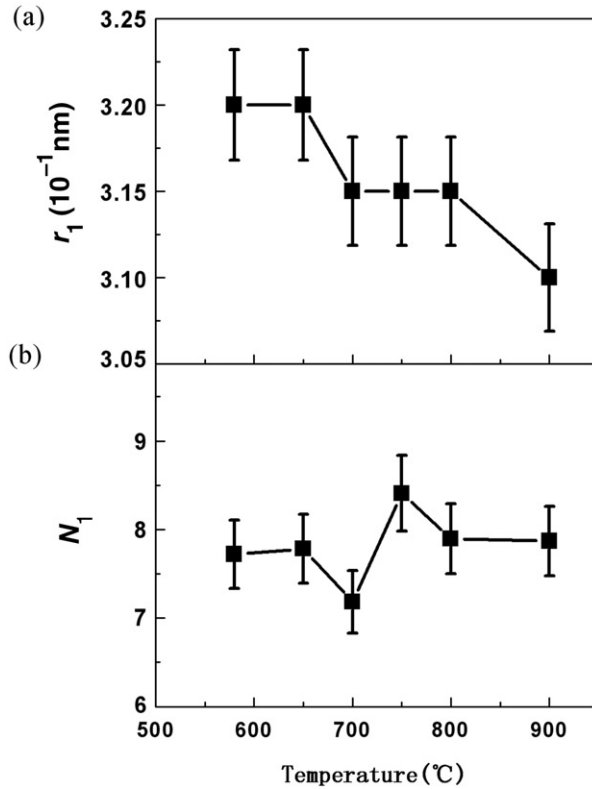
Figure 3. Temperature dependences of r_1 and N_1 of InSn49.1 alloy: (a) mean nearest neighbour distance, r_1, here r_1 corresponds to the position of the maximum of first peak in $g(r)$; (b) coordination number, N_1. The uncertainty limit of the measurement is: $r_1 \sim 1\%$, $N_1 \sim 5\%$.

both the 650–700 and 800–900°C ranges, but we also could not exclude the other possibility that r_1 decreased gradually within error bars. However, we may determine that whether r_1 decreased abruptly within those temperature ranges or not using other methods.

The variation in physical properties is the external representation of the structural change of the melt [17], and conversely, the structure change of the liquid would lead to the variation of physical properties. Therefore, we can judge whether the liquid structure experiences a sudden change or not by investigating the physical properties of the melt. Figure 4 shows the temperature dependences of physical properties (internal fiction, electrical resistivity and thermopower) of InSn49.1 melt in a wide temperature range above liquidus. There is a notable peak on the Q^{-1}–T curve around 760°C, which is hundreds of degrees above the melting point. The ρ–T curves exhibit a non-linear manner within 620–860°C, which is in good agreement with the results of another study [18]. The thermopower of the melt also increases non-linearly with the elevation of temperature, and the temperature range with anomalous change resembles well that seen in internal friction and resistivity measurement. As mentioned above, because the variation in physical properties is the external representation of the structural change, the sudden changes on
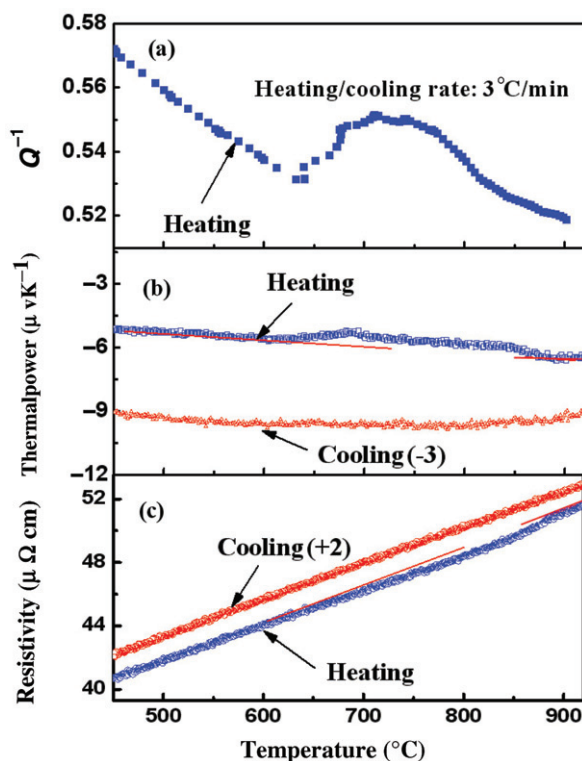
Figure 4. Physical properties (internal fiction Q^{-1}, electrical resistivity ρ and thermopower S) as functions of temperature for liquid InSn49.1 alloy: (a) $Q^{-1} - T$; (b) $S - T$; (c) $\rho - T$ curve. Heating/cooling rate: $3°C/\text{min}^{-1}$.

the curves of Q^{-1}–T, ρ–T and S–T within a similar temperature range imply that the structural features of the InSn49.1 melt changed discontinuously.

   With respect to the liquid structures, as we have mentioned, the structures of some liquid pure metals and alloys may be microheterogeneous at the temperature not far from its liquidus, and there exists a lot of 'short-range ordering domains/microdomains' which are inherited from the initial material. The main parameters used to describe the statistically averaged size of microdomains are the correlation radius r_c and the atom numbers N_c, which vary with the structural change due to the alteration of atomic interaction. As shown in Figure 5, r_c and N_c dropped gradually with temperature increasing till to 800°C; however, both of them dropped sharply between 800°C and 900°C. $\zeta(=r_c/r_1)$ represents the ordering degree of the liquid structure. It changed a little with temperature increasing up to 800°C, but it also decreased evidently within 800–900°C. These results are similar to those we had observed in the InSn80 melt, which suggest obviously that the melt becomes more homogeneous and the microdomain size reduced a lot after the structure change ended.

   The phase diagram of In–Sn alloy [19] shows that the eutectic structure is composed of a β-phase (In-rich) and γ-phase (Sn-rich) in solid state, so it is reasonable to assume that there are two types of microdomains (In-enriched microdomains, Sn-enriched micro-domains) at the temperature not far above the liquidus. Within these microdomains the local microstructures and compositions remain almost constant in spite of long-range
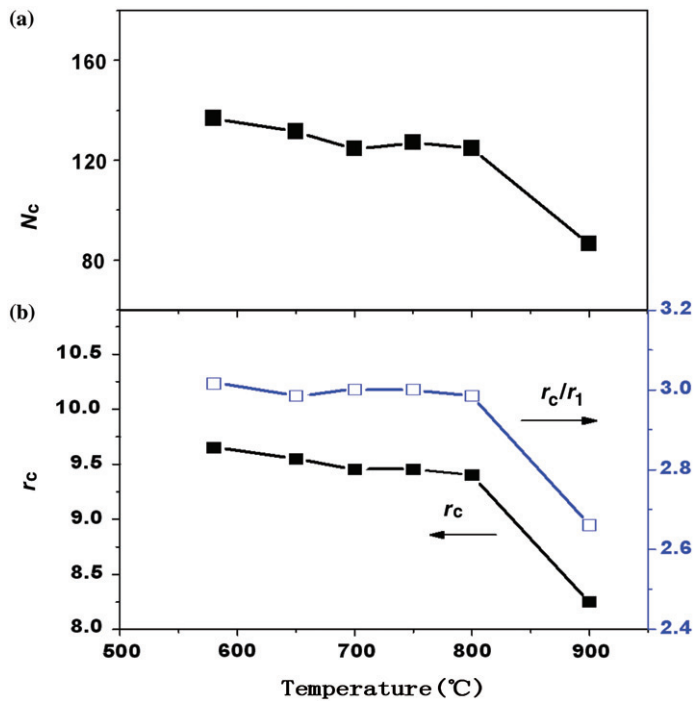
Figure 5. Temperature dependences of N_c and r_c of InSn49.1 alloy: (a) atom number within the orders N_c ($= \int_{r_0}^{r_c} 4\pi\rho_0 g(r)r^2 dr$); (b) the statistically average size r_c of the ordering domain and the ratio r_c/r_1 (ordering degree). r_c can be obtained using a semiempirical approach: $g(r) = 1 \pm 0.02$.

disorders and the energetic undulation. Furthermore, it is known that for tin with covalent bonds in solid state, the residual covalent bonds, namely the short range ordering of tetrahedrons, still exist in the liquid [20–22]. By quantitative analysis of the liquid structures of InSn80 and Sn, Liu et al. [23] believed that Sn plays a crucial role in the discontinuous structure changes of InSn80 melt. Moreover, their findings reveal the structure change happens at 800–1000°C in liquid Sn. Therefore, in this study, it was supposed that the structure change resulted from the adjustment of the atomic bonds of Sn–Sn and In–In. When temperature is elevated above 620°C, the activation energy required for breaking atomic bonds of In–In is high enough to overcome the energy barrier and the In–In bonds are broken continuously. And when temperature increased up to 800°C, Sn–Sn bonds are broken; at the same time, new bonds are built up and a relatively uniform melt is formed.

Now let us see how melt structure changes affect the physical properties of the melt. According to the Nearly Free Electron model (NFE) [24], the resistivity ρ of liquid alloys is given by $\rho = \hbar k_f / n_e e^2 L_0$, where $\hbar$ is the Planck constant, n_e and e are the electron density and charge, respectively. Symbols k_f and L_0 are the Fermi wave number and mean-free path of conduction electrons, respectively. Base on the NFE model, it can be logically assumed that the unusual change of resistivity in InSn49.1 melt was attributed to the big change of n_e and L_0. When the alloy was heated to the critical point, the short-range orders were broken and a new more disordered structure formed. This structure change included

the altering of the nearest neighbour distance, and an abundant release of free electrons, etc., which result in the increasing of n_e and decreasing of L_0 so as to cause the unusual change of the resistivity with temperature increasing.

It is known that at high temperature the thermopower is mainly determined by its diffusive component, and according to electro-transport properties, the thermopower S at the Fermi level can be expressed as

$$S(T) = \frac{\pi^2 k^2}{3|e|} T \left\{ \frac{\partial \ln \rho}{\partial E} \right\}_{E_F},$$

where k is the Boltzmann constant. It shows that with the abnormal changing of the liquid structure, the thermopower also changed non-linearly.

Internal friction, as a structurally sensitive technique, has been widely used for studying structures, crystal defects and phase transitions in solids. Similar to internal friction measured in solid materials, the physical essence of internal friction measured in liquid represents the relative energy dissipation induced by the damping effect of the liquid. In the present study, the sample was subjected to a stress varying in a sinusoidal manner with time, which led to the strain varying in the same manner. Generally speaking, for a completely elastic sample, the stress and strain are in-phase, but for a viscoelastic sample, such as liquid InSn49.1 alloy, the viscous component would cause the stress and strain to be out of phase, i.e. there is a phase lag between them, and lead to the energy dissipation.

However, up to now, the relationship between liquid structure and energy dissipation still not fully understood; in the present article, we attempted to discuss it from another viewpoint. The structure of the improved torsion pendulum internal friction apparatus (see Figure 1 in [14]) used in this experiment is similar to the torsional oscillation viscometer, just the different measurements show the different physical quantities, but both energy dissipation and viscosity related to the viscous resistivity. The relationship between relative energy dissipation Q^{-1} and viscosity η can be presented as [25]:

$$Q^{-1} = \frac{\eta \omega}{\sqrt{A^2 - \eta^2 \omega^2}}, \tag{1}$$

where $\omega = 2\pi f$ is angular frequency, A is apparatus constant, and viscosity η can be presented as:

$$\eta = \frac{2KT}{\delta^3} \tau_0 \exp\left(\frac{U}{KT}\right), \tag{2}$$

where T is the temperature, τ_0 is the vibration period of the atom at equilibrium position (10^{-13} s for liquid metal), U is the activation energy which reflects the strength of interatomic bonding force, and δ is the interatomic distance (generally speaking, $\delta \approx r_1$ [26]). Therefore, relative energy dissipation can be expressed as:

$$Q^{-1} = \left(\frac{A^2}{\omega^2} \frac{\delta^6}{4K^2 \tau_0^2 T^2} \exp\left(-\frac{2U}{KT}\right) - 1 \right)^{-1/2}. \tag{3}$$

It can be seen from Equation (3) that the anomalous variation of the relative energy dissipation might result from the alterations of interatomic distance and activation energy.

4. Conclusions

By means of X-ray diffractometer, internal friction, resistivity and thermopower measurements, a discontinuous temperature-induced liquid–liquid structure change was observed in the heating procedure of the InSn49.1 melt within the temperature range of 620–850°C. Based on the XRD results, it is assumed that the structure change results from the adjustment of the atomic bonds of Sn–Sn and In–In, and this structure change results in the sudden changes of physical properties of the InSn49.1 melt.

References

[1] P.W. Anderson, Science **267**, 1615 (1995).
[2] A.P. Sokolov, Science **273**, 1675 (1996).
[3] P.S. Popel, M. Calvo-Dahlborg, and U. Dahlborg, J. Non-crystal. Solids **353**, 3243 (2007).
[4] U. Dahlborg, M. Calvo-Dahlborg, P.S. Popel, and V.E. Sidorov, Eur. Phys. J. B. **14**, 639 (2000).
[5] E.G. Jia, A.Q. Wu, L.J. Guo, C.S. Liu, W.J. Shan, and Z.G. Zhu, Phys. Lett. A **364**, 505 (2007).
[6] P.S. Popel, O.A. Chikova, and V.M. Matveev, High Temp. Mater. Process. **14**, 219 (1995).
[7] U. Dahlborg, M. Besser, M. Calvo-Dahlborg, G. Cuello, C.D. Dewhurst, M.J. Kramer, J.R. Morris, and D.J. Sordelet, J. Non-crystal. Solids **353**, 3005 (2007).
[8] M. Dutkiewicz and E. Dutkiewicz, Electrochim. Acta **51**, 2346 (2006).
[9] S. Mudry and I. Shtablavyi, J. Non-crystal. Solids **352**, 4287 (2006).
[10] S.V. Prokhorenko, High Temp. **43**, 700 (2005).
[11] F.Q. Zu, Z.G. Zhu, L.J. Guo, X.B. Qin, H. Yang, and W.J. Shan, Phys. Rev. Lett. **89**, 125505 (2002).
[12] F.Q. Zu, X.F. Li, L.J. Guo, H. Yang, X.B. Qin, and Z.G. Zhu, Phys. Lett. A **324**, 472 (2004).
[13] F.Q Zu, Z.G. Zhu, L.J. Guo, B. Zhang, J.P. Shui, and C.S. Liu, Phys. Rev. B **64**, 180203 (2001).
[14] F.Q. Zu, L.J. Guo, Z.G. Zhu, and Y. Feng, Chin. Phys. Lett. **19**, 94 (2002).
[15] F.Q. Zu, Y. Xi, R.R. Shen, X.F. Li, Y. Zhang, and Z.H. Chen, Phys. Chem. Lid. **44**, 543 (2006).
[16] Q. Wang, K.Q. Lu, and Y.X. Li, Acta Phys. Sin. **50**, 1355 (2001).
[17] S.J. Cheng, X.F. Bian, J.X. Zhang, X.B. Qin, and Z.H. Wang, Mater. Lett. **57**, 4191 (2003).
[18] R.R. Shen, F.Q. Zu, Q. Li, Y. Xi, X.F. Li, G.H. Ding, and H.M. Liu, Phys. Scr. **73**, 184 (2006).
[19] T.B. Massalski, *Binary Alloys Phase Diagrams* (American Society for Metals, Metals Park, OH, 1993), Vol. 3.
[20] Y. Kita, J.B. Van Zytveld, Z. Morita, and T. Iida, J. Phys. Condens. Matter. **6**, 811 (1994).
[21] Y. Waseda, *The Structure of Non-crystalline Materials* (McGraw-Hill, New York, 1980).
[22] C.A. Poole, T. Grande, and P. McMillan, Science **275**, 322 (1997).
[23] C.S. Liu, G.X. Li, Y.F. Liang, and A.Q. Wu, Phys. Rev. B **71**, 064204 (2005).
[24] T.E. Faber, *An Introduction to the Theory of Liquid Metals* (Cambridge University, Cambridge, London, 1972).
[25] F.Q. Zu, PhD thesis, Institute of Solid State Physics, Chinese Academy of Sciences, Hefei, 2002.
[26] Y. Zhao, PhD thesis, Shandong University, Jinan, 2007.